

# Optimum Design of a Savonius VAWT for Implementation in Urban Places having Low to Medium Wind Velocities

Animesh Dutta<sup>1</sup>, Harshvardhan Singh<sup>1</sup>, Gaurav Kumar Rai<sup>1</sup> and Anirban Bose<sup>1\*</sup>

<sup>1</sup>Department of Mechanical Engineering, Meghnad Saha Institute of Technology, Kolkata, India

**Abstract.** The deployment of horizontal-axis wind turbines is restricted to specific locations, as their functionality is contingent upon the presence of high-velocity wind conditions. The vibrations and acoustic emissions generated by these massive apparatuses are generally considered unpleasant. Furthermore, the operational expenses associated with these machines are considerably elevated. A significant drawback of this turbine design is the mortality rate of avian species resulting from inadvertent collisions with the rapidly rotating blades. This study presents a viable, albeit not entirely novel, proposition for the implementation of vertical axis wind turbines (VAWT). While it is acknowledged that VAWT may not generate power at the same magnitude as their horizontal counterparts, their application has the potential to satisfactorily fulfill the energy requirements of the region. In urban settings where the installation of large turbines is impractical, VAWT can be readily employed, as they only necessitate low to moderate wind speeds. The operational costs are minimal, and the energy output is capable of meeting the demands of individual buildings or public lighting systems. Enhancements in performance have been examined, leading to the optimization of several design parameters. The ultimate objective is to develop an optimal VAWT design that surpasses the performance of earlier models and is suitable for use in urban environments where wind velocities fluctuate within the low to medium range.

## 1 Introduction

Wind turbines capture kinetic energy from atmospheric wind currents, representing one of the most economically viable energy sources currently accessible. Based on the orientation of the rotor's axis, turbines can be classified into two primary categories: vertical axis wind turbines (VAWTs) and horizontal axis wind turbines (HAWTs). Generally, HAWTs exhibit a superior power coefficient in comparison to VAWTs, thus enabling them to harness a significant quantity of wind energy. Nevertheless, the efficacy of HAWTs is predominantly restricted to areas that experience medium to high wind velocities. Furthermore, these turbines necessitate a more extensive spatial footprint and possess greater height, which contributes to elevated material expenditures and overall financial outlay. In addition,

---

\* Corresponding author: [anirban.bose@msit.edu.in](mailto:anirban.bose@msit.edu.in)

HAWTs present a potential hazard to avian species as they interfere with flight trajectories, resulting in mortality incidents. Given these constraints, HAWTs are deemed unsuitable for urban settings characterized by low to medium wind speeds.

Though traditionally less efficient than HAWTs, VAWTs were created to solve these issues. VAWTs have a lot of potential for urban applications, including high-rise building rooftops, even with their lower efficiency. Due to the paucity of research on VAWTs, it is imperative that these turbines be investigated, designed, and installed in urban environments. The two main categories of VAWTs are lift-based and drag-based. Drag-based VAWTs, like the Savonius rotor, have a maximum tip speed ratio (TSR) of 1, which limits their angular velocity but provides enough torque for good self-starting capabilities. On the other hand, lift-based VAWTs, such as the H-rotor and Darrieus designs, achieve lower torque outputs and faster rotor speeds, but they have poor self-starting characteristics as power generation depends on torque and rotor velocity, both of which are important. Various designs, modifications, and hybrid systems have been developed and investigated by researchers to maximize power generation from variable-angle wind turbines.

[1] A. Al-Faruk and A. Sharifian conducted an experimental study focused on the geometric optimization of a previously proposed configuration known as the Swirling Savonius rotor. Their findings indicated that the optimized parameters, which enhanced the power coefficient, included a blade overlap ratio of 0.2, a hot air inlet diameter of 16 mm, blades with an arc angle of  $195^\circ$ , and a closed top for the swirling chamber. D. D. P. Tjahjana et al. [2] explored the impact of an outer diffuser guide vane (ODGV) design on the performance of Savonius wind turbines. Their results demonstrated a 41.34% improvement in the power coefficient at a wind angle of  $60^\circ$ . For urban applications, the Savonius wind turbine equipped with ODGVs offers advantages such as high torque, stability, low noise levels, effective self-starting capabilities, and ease of manufacture. T.-Y. Chen and Y.-Y. Chen [3] introduced the Vortical Stator Assembly (VSA) design aimed at enhancing the efficiency of drag-type vertical axis wind turbines (VAWTs). Their optimized configuration includes six guide vanes with a VSA diameter approximately 1.82 times that of the rotor diameter. This ideal VSA model was shown to increase the rotor's angular velocity by 318%, output torque by 200%, and maximum power generation by 910% at a wind speed of 6 m/s, resulting in a starting wind velocity for the VSA-integrated turbine of approximately 1 m/s. K. Irabu and J. N. Roy [4] proposed the use of a guidebox tunnel to enhance the effectiveness of the Savonius rotor. This rectangular guidebox, positioned with the rotor at its center, features air inlets and outlets at either end to facilitate wind flow. The optimal area ratio between the entrance and exit of the guidebox was found to be between 0.3 and 0.7 to maximize rotor angular velocity. Additionally, N. C. Uzarraga-Rodriguez et al. [5] investigated the effect of blade count on the aerodynamic performance of rooftop and Savonius rotors. For rooftop rotors, an increase in blade count corresponded to an increase in power coefficient; conversely, the power coefficient for Savonius rotors decreased with more blades. Both rotor types exhibited similar aerodynamic performance at low tip speed ratios (TSR), while rooftop rotors outperformed Savonius rotors at high TSRs. It was also found that four-bladed geometries performed better for rooftop rotors, whereas two-bladed configurations excelled for Savonius rotors. Wind speed significantly influences the power that VAWTs can harness, and various arrangements can be employed to enhance velocity. K. Kołodziejczyk et al. [6] studied the influence of guided vanes on power output, revealing substantial effects on pressure, velocity, torque, and overall power. The optimal torque and power output were achieved with blade angles between  $45^\circ$  and  $55^\circ$ . K. Watanabe et al. [7] presented an innovative approach to increase wind velocity through the use of a wind lens, which combines diffuser elements with flanges. They found that increasing the entering wind velocity markedly improved efficiency. Compared to an uncovered wind turbine, power output doubled with a flat-panel diffuser and increased by a factor of 2.1 with a curved surface

diffuser. Furthermore, as the semi-open angle of the diffuser increased from  $5^\circ$  to  $20^\circ$ , a notable rise in power output was observed. The optimal length for flat-panel diffusers was determined to be  $0.5D$ , with a semi-open angle of  $20^\circ$ . Results indicated that the most effective wind lens design featured a Venturi structure, shorter flanges, and a bent diffuser. Through a comprehensive review of the existing literature, several research gaps have been identified that must be addressed to facilitate the rapid development and implementation of VAWTs. Initially, the focus will be on the optimal design of a Savonius rotor, followed by the integration of an ODGV (Omni Directional Guide Vanes). Prior to this integration, the ODGV design itself will also be optimized. To mitigate the effects of negative torque, particular attention will be given to reducing turbulence in the existing wind flow and directing it appropriately. The optimization parameters for the ODGV vanes will include the number of blades, aspect ratio, and blade angle.

## 2 Optimum Design of Savonius Rotor

Sigurd Johannes Savonius first designed Savonius rotors, sometimes referred to as S-rotors or Savonius wind turbines, in 1931. This rotor was made up of two semi-cylinders arranged and fixed around a vertical shaft, i.e., axis of rotation, in such a way that it looks like the letter S. These semi-cylinders look like a bucket and are referred to as blades. The working principles of these Savonius rotors are similar to those of a cup anemometer and are called drag-based rotors. This is because these rotors rotate due to the moment created by the drag forces acting on their blades. The tip speed ratio of these rotors is always less than 1 because the linear velocity of the blade tip can never exceed the linear velocity of the incoming wind, as they work as a result of drag forces acting on the blade surface, created by the incoming wind. Savonius' analysis of the performance of approximately thirty different models of S rotors yielded a maximum coefficient of power ( $C_p$ ) of 0.31 from wind tunnel studies and 0.37 from open-air experiments. Several studies conducted thereafter reported  $C_p$  in a range of 0.15 to 0.35 [8].

### 2.1 Working Principle

When wind blows and strikes the surface of the blades of Savonius rotor, due to the drag force, a moment gets created, which in turn rotates the rotor. This drag force is actually proportional to the drag coefficient of the surface on which the wind strikes. More the drag coefficient, the more will be the drag force, and thus the rotor will rotate at a higher speed and with higher torque. Fig. 1. represents a Savonius rotor and how incoming wind strikes the blade surface and causes it to rotate in a clockwise direction. The figure illustrates a double-bladed Savonius rotor, and when the wind strikes at a particular moment, one of the blade faces acts as a concave surface, thus having a higher drag coefficient, whereas the other face acts as a convex surface and thus has a lower drag coefficient. As a result of these different drag coefficients, the torque created would be greater on the face having a higher drag coefficient, i.e., the concave face. The torque created on the concave surface is known as positive torque, whereas the torque created on the convex surface is known as negative torque as it resists the clockwise rotation of the rotor. The torque generated by the convex face is greater than that produced by the concave face, resulting in torque operating on the rotor [9].

## 2.2 Design Parameters

Savonius rotor performance is impacted by a variety of design elements [10]. In this study, we have identified some of the design parameters that significantly influence the performance of Savonius rotors. Those design parameters are the number of rotor blades and aspect ratio. Two, three and four numbers of blades shall be taken and analysed for their performance analysis. For aspect ratio, two bladed rotors shall be taken, and different values of aspect ratio such as 0.5, 1.5, 2, 4, and 5 shall be analysed. The height to diameter of the rotor is what is referred to as the aspect ratio. The shape of the rotor blade is fixed as a semi-cylindrical shape because previous studies have already reported that this shape gives better performance compared to the others [11]. The objective of this research is to optimise the design of the Savonius rotor by finding out the optimum values of the above-mentioned design parameters. At such optimum values, this rotor would be able to extract maximum power from the incoming wind. This optimisation would be done with reference to the power coefficient ( $C_p$ ) and torque coefficient ( $C_t$ ).

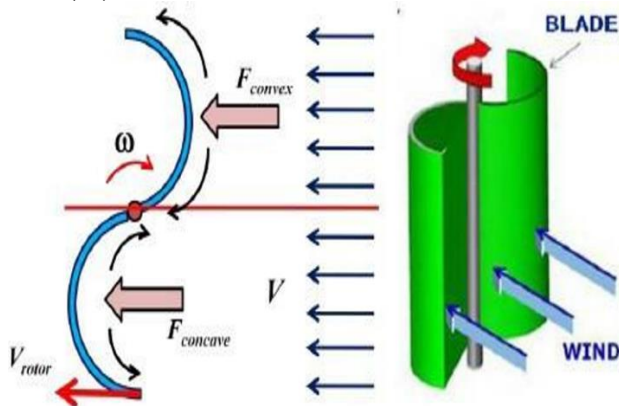
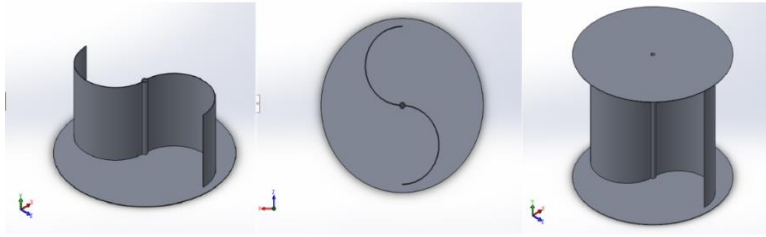


Fig. 1. Working principle of Savonius rotor

The ratio of the wind turbine's actual power to all the wind power entering the turbine blades at a given wind speed is known as  $C_p$ . The ratio of the actual torque generated by a wind turbine to the entire torque that the wind is able to generate is known as  $C_t$ , on the other hand. The maximum values of  $C_p$  and  $C_t$  must be present in the optimal design parameter values.

## 2.3 Modeling and Analysis

The CAD model of the savonius rotor was made in SOLID-WORKS. Different CAD models having different numbers of blades were made. Different views of these CAD models have been shown in Fig. 2, 3, and 4.



**Fig. 2.** Two-bladed Savonius rotor (from left: isometric section view, top section view, isometric view)

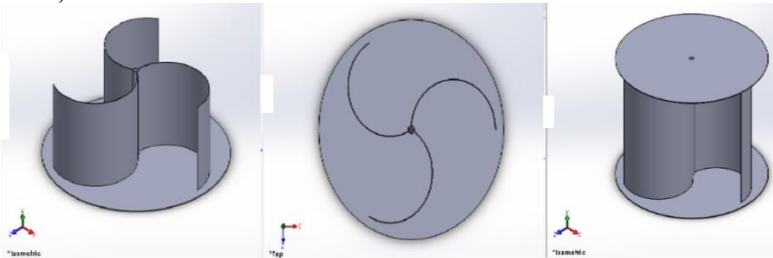


**Fig. 3.** Three-bladed Savonius rotor (from left: isometric section view, top section view, isometric view)

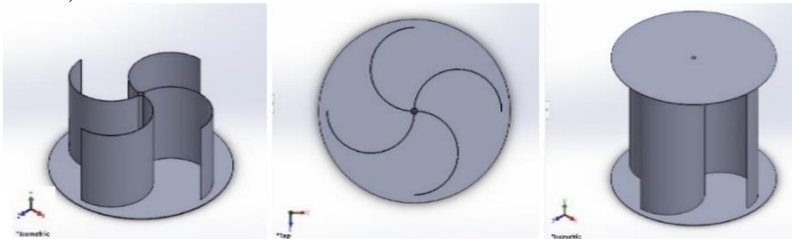


**Fig. 4.** Four-bladed Savonius rotor (from left-isometric section view, top section view, isometric view)

These CAD models were then converted into parametric files and uploaded in ANSYS Workbench. Simulations were then performed on these CAD models in ANSYS Student 2021 R2. CFX solver was used, and transient state analyses were performed on these models. The K- $\epsilon$  turbulence model was used to perform the CFD analyses. These analyses were performed for four different incoming wind velocities, i.e., 2, 4, 6, and 8 m/s. For every incoming wind velocity, the corresponding maximum angular velocity and maximum net torque were calculated. The product of these two gives us the maximum power of the wind turbine. Now, having these data, we will further calculate the wind power, rotor power,  $C_p$ , wind torque,  $C_t$ , and TSR.

$$TSR(\lambda) = \frac{v_{rotor}}{v} = \frac{\omega r}{v} \quad (1)$$

$v_{rotor}$ =linear velocity of the rotor tip;  $\omega$ =angular velocity of the rotor;  
 $v$ =velocity of the incoming wind;  $r$ =radius of the rotor

$$C_t = \frac{T}{T_W} = \frac{2T}{\rho A_S r v^2} \quad (2)$$

$T_W$ =wind torque,  $T$ =torque,  $\rho$ =density,  $A_s$  = swept area of blade = rotor height  $\times$  rotor diameter

$$C_p = \frac{P_t}{P_W} = \frac{2T\omega}{\rho A_s v^3} \quad (3)$$

$P_t$ =maximum power on the rotor,

$P_W$ =power of the incoming wind striking blades of the rotor

Also, the same analysis is repeated for studying the effect of aspect ratio on the  $C_p$  value. For this, different values of aspect ratio are taken for study, such as 0.5, 1.5, 2, 4, 5. For each of these aspect ratios, the TSR and  $C_p$  are determined.

### 2.4 Results and Discussion

After performing all the simulations, the calculated data was recorded, and various plots of those data have been presented and discussed in this section. For an approaching wind velocity of 8 m/s in the positive x-direction, contour plots of the variables eddy viscosity, pressure distribution, and velocity are shown in Fig. 5, 6 and 7 for two, three, and four bladed Savonius rotors, respectively.

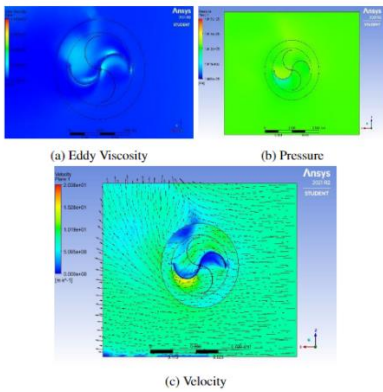


**Fig. 5.** Contour plots of two bladed Savonius rotor

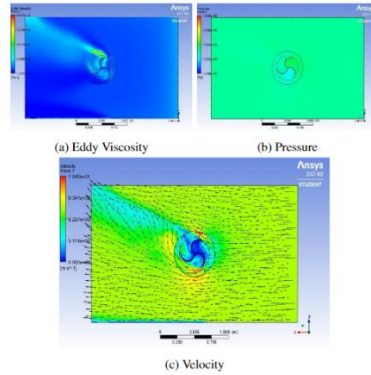


**Fig. 6.** Contour plots of three bladed Savonius rotor

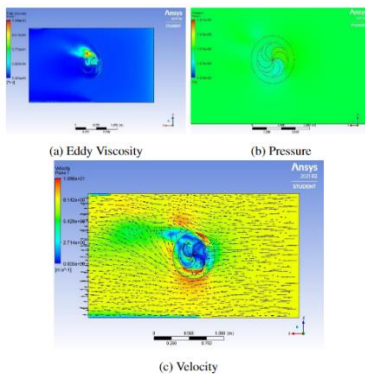


**Fig. 7.** Contour plots of four bladed Savonius rotor

Now, performance plots for  $C_p$ ,  $C_t$  and angular velocity of rotor vs. wind velocity shall be presented below for two (Fig. 8 and Fig. 9), three (Fig.10 and Fig.11), and four bladed (Fig.12 and Fig.13) Savonius rotors.

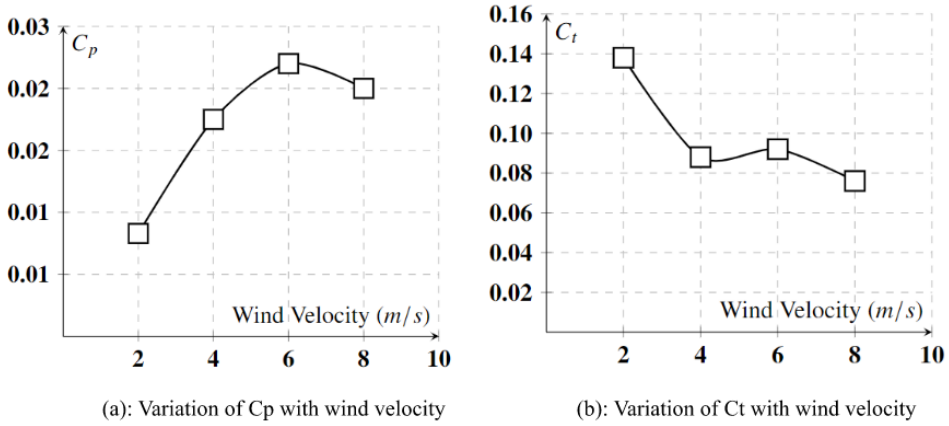


**Fig. 8.** Performance of two bladed Savonius rotor

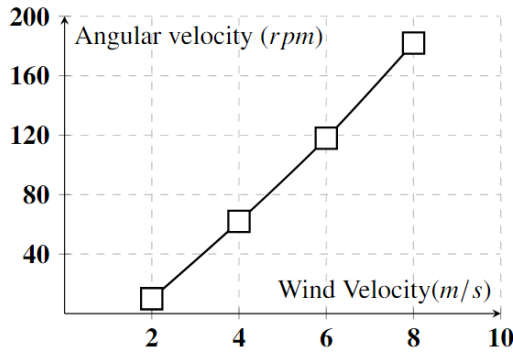


**Fig. 9.** Angular velocity of two bladed Savonius rotor with wind velocity

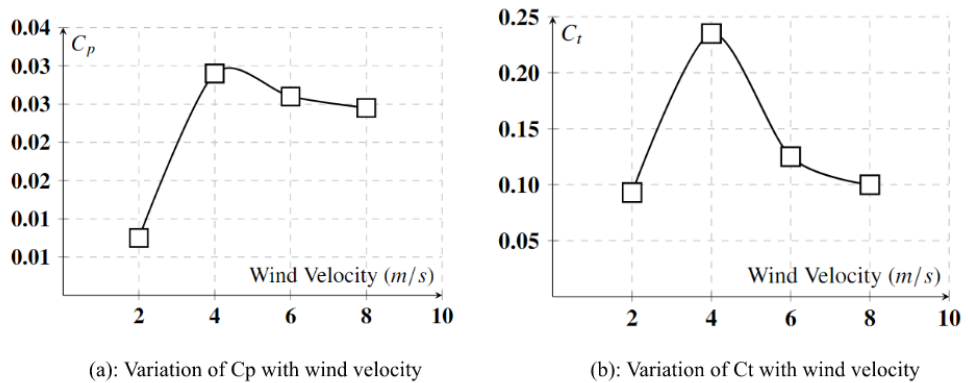


**Fig. 10.** Performance of three bladed Savonius rotor

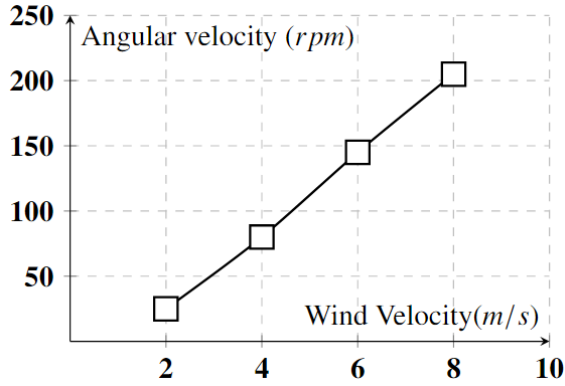


**Fig. 11.** Angular velocity of three bladed Savonius rotor with wind velocity

As it can be observed, in a two-blade Savonius rotor, maximum  $C_p$  occurs at a wind velocity of 6 m/s, and beyond that, it starts decreasing due to the increased turbulence of air as it strikes the blade surface. Also, in this case, the power output is not stable because when the blades become parallel to the blowing wind, minimum torque is formed. For a three-blade rotor, maximum  $C_p$  and  $C_t$  occur at a wind speed of 4 m/s, and also power output is stable in this case. For four-bladed rotors as well, maximum  $C_p$  and  $C_t$  occur at a wind speed of 4 m/s, and these values are actually maximum among all the data for two, three, and four-bladed Savonius rotors.

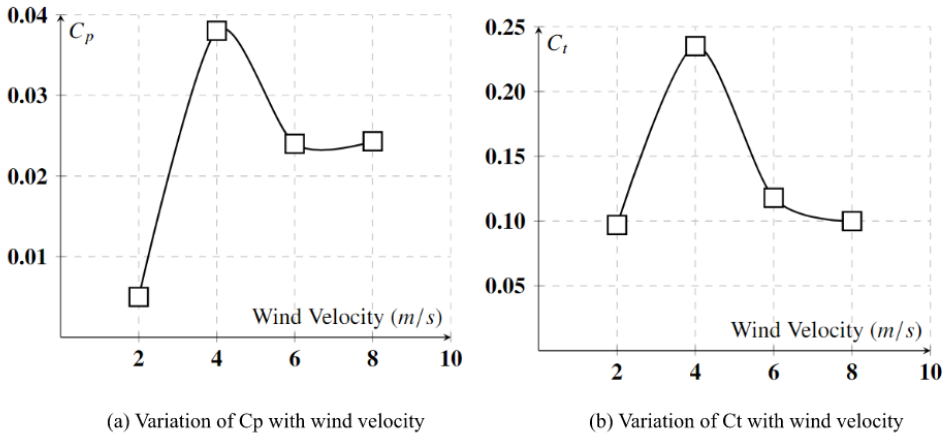


**Fig. 12.** Performance of four bladed Savonius rotor



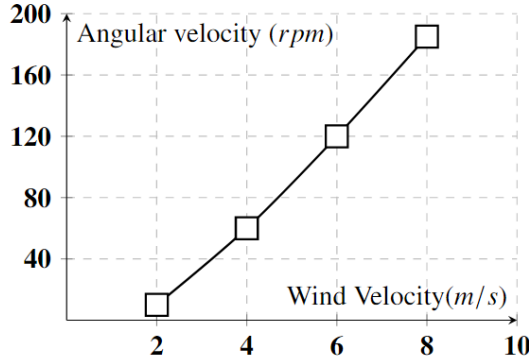


**Fig. 13.** Angular velocity of four bladed Savonius rotor with wind velocity

On observing the angular velocity of rotor vs. wind velocity plots of different rotors, it is inferred that maximum rotations per minute are obtained in three-bladed rotors, and also that of the two bladed rotor is very close to that value. Therefore, it is clear that at a given wind speed, the angular velocity of a four-bladed rotor is significantly lower than that of two-bladed and three-bladed rotors. As can be shown, the maximum  $C_p$  for a two-bladed Savonius rotor occurs at a wind speed of 6 m/s, and after that it begins to decrease as a consequence of the increased turbulence of the air hitting the blade surface. Also, in this case, the power output is not stable because when the blades become parallel to the blowing wind, minimum torque is formed. So, for single-use applications, a three-bladed Savonius rotor is advised since it provides good angular velocity, enough torque, and reliable power production. If a two-bladed Savonius rotor is to be used alone, it must have some special arrangements, such as the implementation of ODGV around the rotor, to get satisfactory performance. Fig. 14 and Fig. 15 present a plot of  $C_p$  vs. TSR and  $C_t$  vs. TSR for two, three, and four-bladed Savonius rotors, and it can be observed in this graph that a three-bladed rotor gives a stable power output without sharp variations in  $C_p$  or  $C_t$ . Fig. 16 shows a plot of  $C_p$  vs. aspect ratio at a constant TSR of 0.5.

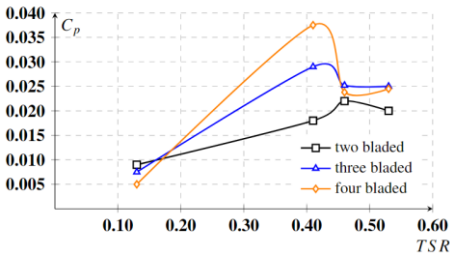


**Fig. 14.** Variation of  $C_p$  with TSR for Savonius rotors

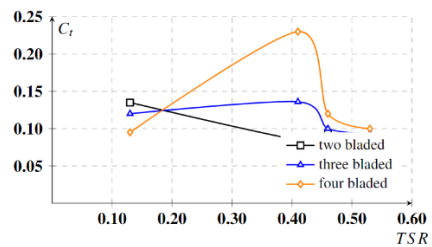


**Fig. 15.** Variation of  $C_t$  with TSR for Savonius rotors

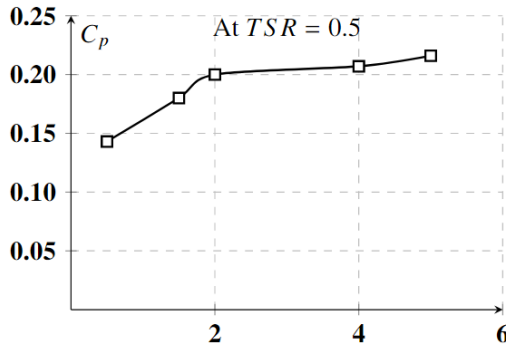


**Fig. 16.** Variation of  $C_p$  with aspect ratio

As it can be observed in the above graph,  $C_p$  has not increased much after aspect ratio 2 because now, with further increase in aspect ratio, friction also increases, which will eventually decrease the power output. Thus, the value of the aspect ratio should lie between 1 and 2 for better performance of the rotor.

### 3 Integration of ODGV in Savonius Rotors

ODGVs, known as Omni Direction Guide Vanes, are an innovative device that surrounds a VAWT, designed and developed to improve the rotor performance [12]. This performance improvement signifies that on integrating these ODGVs in Savonius and H rotors, there is a significant increment in the power output of the rotor. ODGVs have several static vanes inclined at an angle, known as the blade angle. An example of it is shown in the Fig. 17 below. As it can be seen, the stator vanes are arranged in a way that it captures the blowing wind and directs them in a particular direction, thereby reducing any previous turbulence [13]. When wind blows in the surrounding area, it often has a lot of turbulence, which makes it difficult for the wind turbine to efficiently extract wind power. With the implementation of these ODGVs around the wind turbine, the above-mentioned problem can be overcome. Additionally, since the wind is directed in a specific desirable direction to limit turbulence, the adverse torque on the convex surface is also reduced, enhancing the net torque and angular velocity of the rotor. Also, the design of these ODGVs is aesthetically friendly.

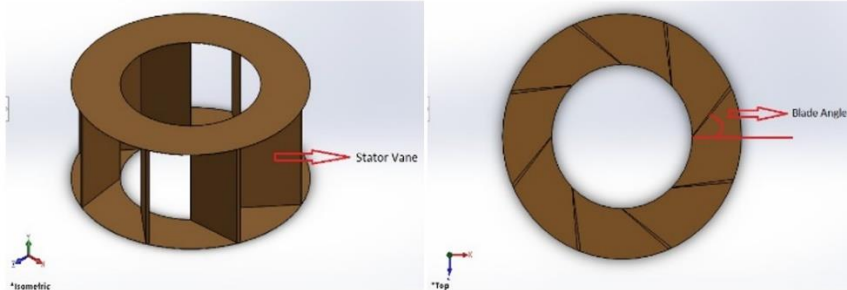


**Fig. 17.** Eight bladed ODGV (Left: Isometric view; Right: Top view)

#### 3.1 Design Parameters and Analysis

In our study, we have opted for eight-bladed ODGV, as it is already known from the available literature that it has better performance than the rest. Our design parameter in this case is the blade angle of the static vanes of the ODGV. Different blade angles such as  $0^\circ$ ,  $20^\circ$ ,  $40^\circ$ ,  $60^\circ$ ,

and  $80^\circ$  have been considered for this analysis. The inner diameter of this ODGV is selected as 500 mm and the outer diameter as 900 mm, whereas the height is 400 mm. For performing this analysis, two bladed Savonius rotor was selected. The CAD models were formed in Solidworks and then converted into parametric files and uploaded in ANSYS Workbench. Simulations were then performed on these CAD models in ANSYS Student 2021 R2. CFX solver was used, and transient state analyses were performed on these models. The  $K - \epsilon$  turbulence model was used to perform the CFD analyses. This way, the optimum blade angle shall be identified, which will correspond to the maximum  $C_p$  value.

### 3.2 Results and Discussion

In this section, we shall focus on the analyses performed on the ODGV integrated two bladed Savonius rotor. By observing the obtained data, we shall comment on the feasibility of using ODGV and also what blade angle is optimum to maximise the coefficient of power  $C_p$ . In Fig.18 , an ODGV-integrated Savonius rotor has been shown.

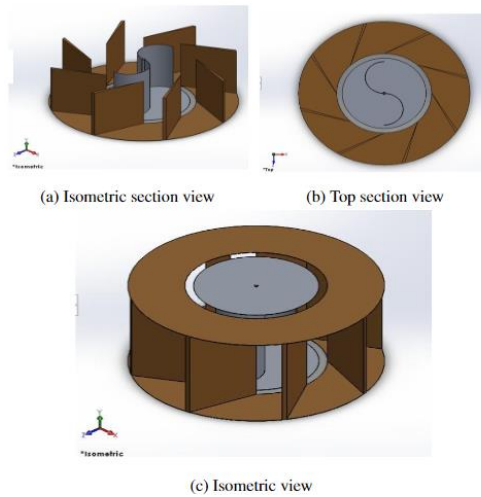


**Fig. 18.** ODGV integrated Savonius rotor

After performing all the simulations, the calculated data was recorded and various plots of those data have been presented and discussed in this section. For an entering wind speed of 8 m/s in the positive x-direction, the contour plots of eddy viscosity, pressure distribution, and velocity are shown in the Fig.19. As it can be seen in the contour plot of velocity, there is a slight reduction in velocity once the wind enters the static vanes of ODGV, and hence a rise in pressure.

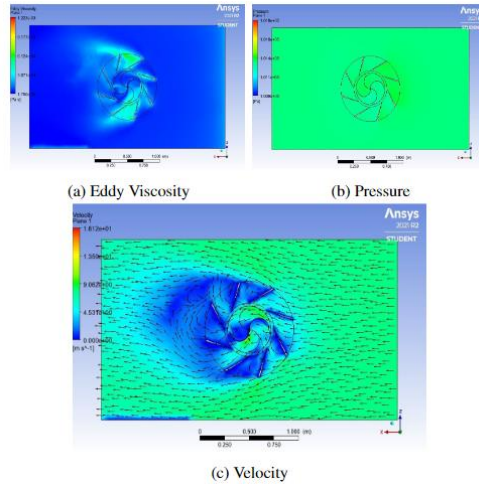


**Fig. 19.** Contour plots of ODGV integrated Savonius rotor

As it is observed in the Fig. 20, at a blade angle of  $60^\circ$ , the values of  $C_p$  and  $C_t$  are 0.279 and 0.1607 respectively, which is the maximum. Thus, we can conclude that  $60^\circ$  is an optimum blade angle for the ODGV, as it maximises the performance of the wind turbine. Also, it can be seen that  $0^\circ$  blade angle gives the worst performance.

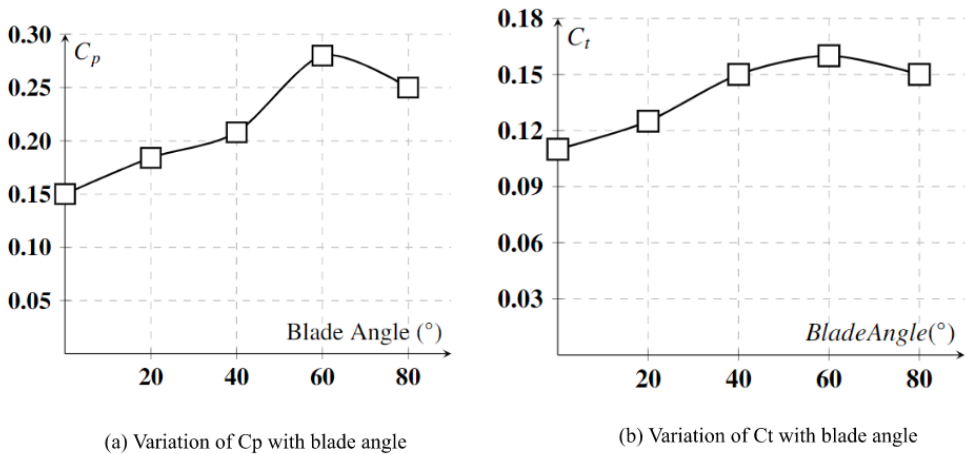


**Fig. 20.** Performance of ODGV integrated Savonius rotor

## 4 Conclusion

Our main focus was to maximise the power output for the VAWT. In this order, various types of wind turbines and their performance parameters have been analysed. It is time to conclude from all those results. It was clear from the test results of the savonius rotors that three-bladed savonius rotors are the best for small-scale VAWT for urban use. It was also seen that angular velocity increased with the number of blades but then decreased for 4-bladed rotors. This was due to turbulence associated with the number of blades. By using ODGV, the torque and the power coefficient have enhanced. It was evident that ODGV boosted the performance of the wind turbine. The aspect ratio for the same has also been discussed and it was concluded that

the aspect ratio for the rotors should be within the limits of 1 and 2. The aspect ratio in the range of 1 to 2 has shown a positive impact on the performance of the wind turbine. It boosted the coefficient of power. The effect of ODGV was also studied and the results showed that ODGV boosted the overall performance of the rotor. By using ODGV, we have seen that the negative torque created by the convex surface reduced and hence it increased the net torque output and power output.

## References

1. A. Al-Faruk and A. Sharifian, Geometrical optimization of a swirling Savonius wind turbine using an open jet wind tunnel, *Alex. Eng. J.* **55**, 2055 (2016).  
<https://doi.org/10.1016/j.aej.2016.07.005>
2. D. D. D. P. Tjahjana, S. Hadi, Y. A. Wicaksono, D. M. Kurniawati, F. Fahrudin, I. S. Utomo, S. I. Cahyono, and A. Prasetyo, Study on performance improvement of the Savonius wind turbine for Urban Power System with Omni-Directional Guide Vane (ODGV), *J. Adv. Res. Fluid Mech. Therm. Sci.* **55**, 126 (2019).  
[http://semarakilmu.com.my/journals/index.php/fluid\\_mechanics\\_thermal\\_sciences/article/view/3058/1726](http://semarakilmu.com.my/journals/index.php/fluid_mechanics_thermal_sciences/article/view/3058/1726)
3. T.-Y. Chen and Y.-Y. Chen, Developing a vortical stator assembly to improve the performance of Drag-type vertical-axis wind turbines, *J. Mech.* **31**, 693 (2015).  
<https://doi.org/10.1017/jmech.2015.35>
4. K. Irabu and J. N. Roy, Characteristics of wind power on Savonius rotor using a guide-box tunnel, *Exp. Therm. Fluid Sci.* **32**, 580 (2007).  
<https://doi.org/10.1016/j.expthermflusci.2007.06.008>
5. N. C. Uzarraga-Rodriguez, A. Gallegos-Munoz, and J. M. Riesco A'vila, *Numerical analysis of a rooftop vertical axis wind turbine*, in *Energy Sustain.* (2011), pp. 2061–2070.  
<https://doi.org/10.1115/ES2011-54173>
6. K. Kołodziejczyk, R. Ptak, and J. Korman, Numerical modeling of vertical axis wind turbine with air guides, *New Trends Prod. Eng.* **2**, 589 (2019).  
<http://dx.doi.org/10.2478/ntpe-2019-0064>
7. K. Watanabe, S. Takahashi, and Y. Ohya, Application of a Diffuser Structure to Vertical-Axis Wind Turbines, *Energies* **9**, 406 (2016).  
<https://doi.org/10.3390/en9060406>
8. K. A. H. Al-Gburi, B. A. J. Al-quraishi, F. B. Ismail Alnaimi, E. S. Tan, and A. H. S. Al-Safi, Experimental and Simulation Investigation of Performance of Scaled Model for a Rotor of a Savonius Wind Turbine, *Energies* **15**, 8808 (2022).  
<https://doi.org/10.3390/en15238808>
9. E. Achdi, S. Syahbardia, and F. F. Rusdianto, Model Design of Helical Type Vertical Shaft Wind Turbine with Capacity of 5 W, *Mestro J. Tek. Mesin Dan Elektro* **5**, 16 (2023).  
<https://doi.org/10.47685/mestro.v5i1.399>
10. S. Osama, M. Emam, S. Ookawara, and M. Ahmed, Enhancing the performance of vertical axis hydrokinetic Savonius turbines using a novel cambered hydrofoil profile for rotor blades, *Ocean Eng.* **292**, 116561 (2024).

- <https://doi.org/10.1016/j.oceaneng.2023.116561>
11. G. V. Babu and D. K. Patel, Effect of Semi-elliptical Outer Blade-surface on the Savonius Hydrokinetic Turbine Performance: A Numerical Investigation, *J. Appl. Fluid Mech.* **17**, (2024).  
<https://doi.org/10.47176/jafm.17.4.2235>
  12. A. Ashmawy, A. Medhat, and M. H. Nasef, Hydrokinetic hybrid vertical axis rotor performance at difference blade shape and angles of attack, *Ocean Eng.* **291**, 116500 (2024).  
<https://doi.org/10.1016/j.oceaneng.2023.116500>
  13. S. A. H. Jafari, K. C. S. Kwok, F. Safaei, B. Kosasih, and M. Zhao, Aerodynamic analysis of a stator-augmented linear cascade wind turbine, *Wind Energy* **22**, 1148 (2019).  
<https://doi.org/10.1002/we.2346>